1-1-1993

Cryogenic Michelson Interferometer on the Space Shuttle

Stan Wellard

Jeff Blakeley

Steven Brown

Brent Bartschi

Cryogenic Michelson interferometer on the space shuttle

Stan Wellard, Jeff Blakeley, Steven Brown, and Brent Bartschi

Space Dynamics Laboratory, Utah State University
Logan, UT. 84322-4140

E. R. Huppi

Geophysics Directorate of the USAF Phillips Laboratory
Hanscom Air Force Base, MA. 01731

ABSTRACT

A helium-cooled interferometer was flown aboard shuttle flight STS-39. This interferometer, along with its sister radiometer, set new benchmarks for the quantity and quality of data collected. The interferometer generated approximately 150,000 interferograms during the course of the flight. Data was collected at tangent heights from the earth's surface to celestial targets. The interferograms encoded spectral data from aurora, earth limb, and earth terminator scenes.

The interferometer collected data at resolutions of 8, 4, and 1 wavenumbers over a spectral range of 2 to 25 micrometers. The interferometer's optics, detectors and preamps, laser reference system, realignment system, and eight-position optical filter wheel are described as they performed on-orbit.

1.INTRODUCTION

The helium-cooled interferometer flown aboard the Space Shuttle *Discovery* as part of the AFP-675 payload has been described in earlier papers[1,2]. This interferometer was part of the Cryogenic Infrared Radiance Instrumentation for Shuttle (CIRRIS 1A) effort. The infrared sensor operated on-orbit from April 28 to May 2 of 1991 as part of the AFP-675 payload.

This paper discusses some of the operational and engineering aspects associated with using an interferometer aboard a space shuttle to collect IR data. Data obtained during the flight is now being processed and presented in other papers[3,4,5]. The successful operation of the C-1A interferometer aboard *Discovery* was the result of a team effort dedicated to optimizing the performance of this instrument and managing its on-orbit environment to assure optimum data collecting conditions.

2.INTERFEROMETER DESCRIPTION

Figure 1 is a functional block diagram of the C-1A interferometer. Figure 2 is a cut-away drawing showing the physical arrangement of the basic interferometer cube. The instrument had an eight-position filter wheel, an optical modulation system that included the moving mirror suspended on its support carriage, a fixed mirror supported by an auto-alignment mechanism, a potassium bromide beamsplitter, and Ritchey-Chretien f/1.6 focal plane optics. The focal plane had five detectors of different sizes with cold preamplifiers. Two redundant laser systems provided spatial sampling of the main channel interferograms. An array of internal IR sources was available for alignment and calibration tracking during flight.

The interferometer design included two electronics units; the Interferometer Control Electronics (ICE), and the Interferometer Signal Conditioning Electronics (ISCE). The ICE processed commands from the Aft Flight Deck (AFD) or from an on-board CIRRIS command sequencer to reconfigure the interferometer for each data take. The ISCE processed the interferogram signals from the five detectors. Data formatting was handled by two redundant Data Formatting Electronics (DFE) units. The DFEs added pertinent housekeeping data as headers to the main channel IR data before it was recorded on two redundant tape recorder systems.

0-8194-0938-3/93/$4.00

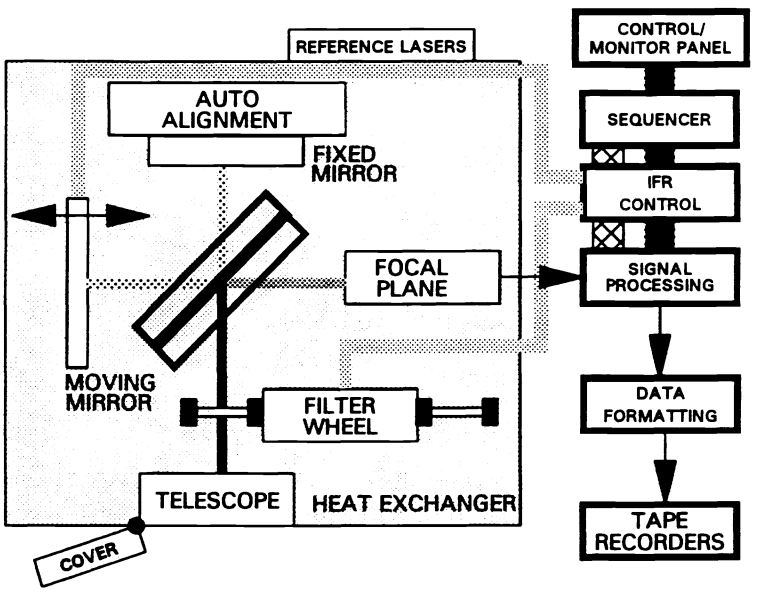

FIGURE 1: CIRRIS 1A Interferometer Block Diagram

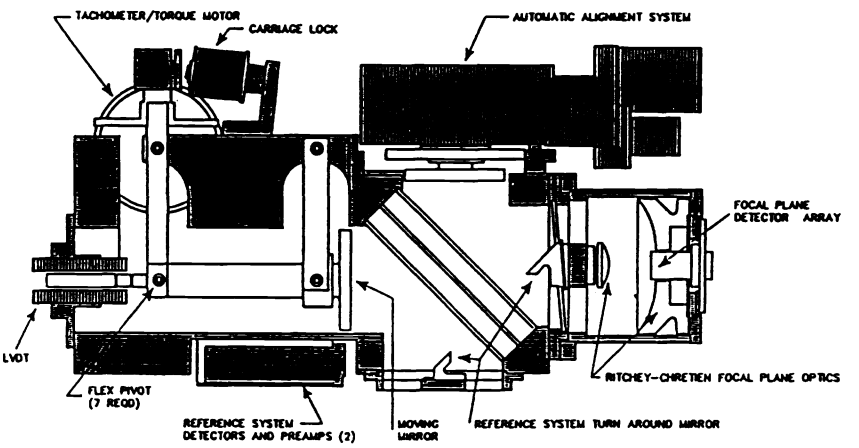

FIGURE 2 Cut away View of CIRRIS 1A Interferometer

2.1 Optical Filter Wheel

The eight-position filter held seven optical filters with one position left open. The filter wheel design allowed bi-directional filter selection and reported absolute wheel position to the AFD and to the DFE for inclusion in the header of each scan.

Filter position 4 provided two functions. An opaque blank, drilled out to transmit approximately 10% of the energy passing through the filter, was combined with a 2.6 to 4.05 μm bandpass filter to limit radiant energy coming from very bright sources. IR energy from the alignment or blackbody source was scattered from the back of this filter and used as a source for alignment checks.

Table 1 is a summary of the characteristics of the eight positions.

TABLE 1. FILTER WHEEL SPECTRAL CHARACTERISTICS

POSITION	DESCRIPTION
0	Open
1	Short Pass ($\leq$4.98 μm)
2	Short Pass ($\leq$3.7 μm)
3	BandPass (4.7 to 13.0 μm)
4	BandPass (2.6 to 4.05 μm) 10% Neutral Density
5	BandPass (11.0 to 13.0 μm)
6	Long Pass ($\geq$17.0 μm)
7	BandPass (8.0 to 13.0 μm)

2.2 Moving Mirror Carriage

The interferometer's moving mirror carriage supported the translating mirror and moved at constant velocity to modulate incoming IR energy. The carriage was a parallelogram structure with seven flex pivots supporting the structural elements of the carriage. The pivots allowed for changes in the parallelogram to convert the rotational motion of the drive motor to the linear back-and-forth movement required for the modulating mirror. The driving DC torque motor was part of a control servo system that moved the mirror at one fixed velocity during scan and another during retrace. Scan velocity was 0.57 mm/sec; retrace velocity was 3.8 mm/sec. Velocity feedback for the servo came from an electromagnetic tachometer. A signal from a Linear Variable Differential Transformer (LVDT) system was used to reverse the direction of the moving mirror to achieve the three resolutions of the interferometer. The moving mirror control subsystem was intended to rapidly reverse the direction of the moving mirror, achieve a constant velocity, and remain at speed in the presence of mechanical or electrical disturbances during the data collection portion of each scan.

Three MMC scan modes (long, medium, and short) were used in the 39 mission modes. These three scan lengths gave approximate resolutions of 1,4, and 8 cm^{-1}, respectively. Interferograms generated were single-sided with about 600 samples on the short side of the Zero Path Difference (ZPD). Table 2 gives scan and retrace periods. The scan and retrace cycle paced experiment operations. Experiment reconfiguration (i.e. changing filter wheel positions, bias, gain, etc.) took place during retrace to minimize interferometer data loss.

TABLE 2. MMC SCAN MODE TIMES

RETRACE (SEC)	SCAN (SEC)	
0.24	Short	1.5
0.42	Medium	2.7
1.5	Long	9.8

2.3 Beamsplitter

Potassium bromide was selected as the material for the beamsplitter to cover the 2.5 to 25 μm range. The material was flat to a quarter wavenumber at 0.6328 μm. The material and its compensator plate were wedged to 20 to 40 arcseconds to reduce channel spectra. ZnSe was used over the reference laser area and Ge over KRS-5 was used in the main area. The potassium bromide beamsplitter was installed in a mount that was both axially and radially spring-loaded to withstand the loads experienced during launch and de-orbit.

2.4 Detectors

The five detectors subtended a field of view of 26.2 mr (1.5°) x 16.5 mr (0.945°). Figure 3 shows the detector arrangement on the focal plane. Four tangent heights are included in the diagram to show the tangent heights at the edges of detectors 1 and 2 when the optical center line was at 90 Km.

Detector size, electronic configuration, and electronic gain and bias gave the interferometer a wide dynamic range. Detectors 1 and 2 provided high sensitivity and high spectral resolution. Detector 2, centered on the optical axis, was the prime detector in the focal plane. Detectors 3, 4, and 5, because of their separation and small size, offered high spatial resolution at moderate spectral resolution and rather low sensitivity. Their low sensitivity, however, increased the instrument's dynamic range. The temperature of the focal plane was controlled at approximately $10 \pm 0.1°$ Kelvin. A closed-loop temperature controller was used to maintain the focal plane's operating temperature. The focal plane was thermally isolated from a heat exchanger, cold strapped to the liquid helium dewar, and then heated to the 10° Kelvin set point with a small resistor. Feedback came from a temperature diode mounted on the focal plane.

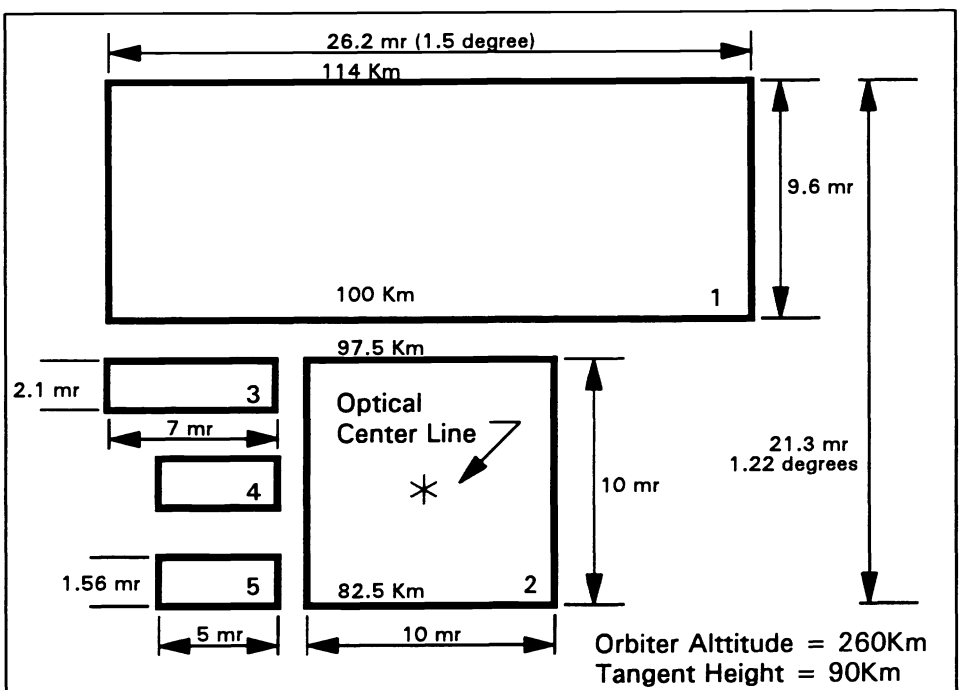

Figure 3: Focal Plane arrangement in Object Space

2.5 Reference Lasers

A redundant mirror position reference system was interfaced with the optical modulator to measure displacement of the mirror and provide spacial sampling of the five main channel interferograms. This system consisted of two fully redundant helium-neon lasers, each with its own fiberoptics channels running from the external lasers to the interior of the heat exchanger that housed the interferometer. The system also included a detector, preamplifier, and signal conditioning for each channel. The reference laser system used the center obscuration feature of the Ritchey-Chretien optics, sending an anti-parallel reference laser beam through the beamsplitter, as shown in Figure 4, to the working reference detector. The laser 1 reference system was selected at power-up.

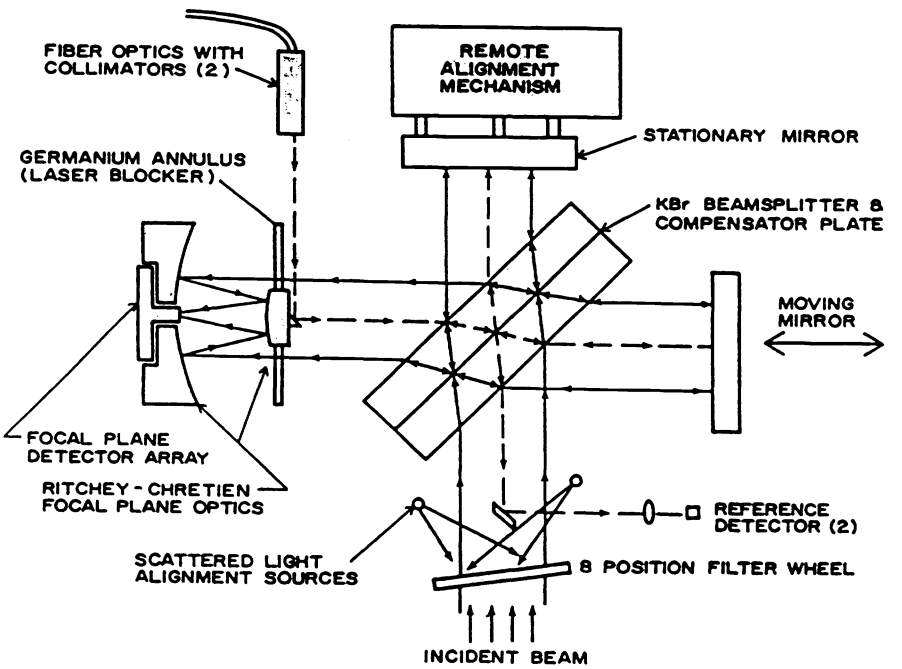

FIGURE 4: Energy Path Through the CIRRIS 1-A Interferometer Optical Modulator

During MMC constant-speed forward scans, the 6328 Å reference laser produced a 1800 Hz zero-crossing reference signal that governed main channel sampling in the ISCE. A laser envelope monitor provided crew members with data on the minimum and maximum laser signal amplitude for any given interferometer scan; these data, in conjunction with laser DC levels and other housekeeping data, were used to monitor the health of the working laser. If the data indicated that the primary laser was malfunctioning, the crew member could switch to subsystem number two. Had both lasers failed, an interferogram sample oscillator provided a final level of redundancy.

2.6 Auto Alignment

The fixed mirror was suspended on a three-point mount connected to the automatic alignment system. For the interferometer to be operational, the fixed and moving mirrors had to be in near-perfect alignment. Alignment can be affected by vibration levels and thermal gradients. If signal levels had decreased below acceptable limits, the crew could have initiated either a "near start" or "cold start" algorithm to restore alignment. "Near start" was available to restore alignment if it was found to be greater than about 8 %. The "cold start" command was reserved for the case where the alignment was found to be less than 8 %.

Stepper motors under microprocessor control could move the fixed mirror via anti-backlash gear trains by moving two points of the mirror mount and moving the mirror to the proper position to re-establish proper alignment. This process would first return the mirror to a known position and then methodically search for a mirror position that increased the value of the interferogram peak signal level at ZPD above pre-programmed values.

2.7 Internal IR Sources

The radiometric accuracy of an interferometer is a function of its optical alignment; and because this alignment is subject to change during flight, the interferometer includes a number of internal sources for alignment and optical performance tracking. The interferometer internal stimulator sources included an alignment source, a blackbody source, two wideband sources (WB1 and WB2), and an off-axis source.

The alignment and blackbody sources were sets of three Chicago Miniature lamps located inside the entrance aperture of them interferometer, just past the position of the current optical filter. The 6 lamps were spaced at 60° intervals around the entrance aperture. The envelopes of the three blackbody lamps were removed to provide long wavelength energy; the envelopes for the alignment source lamps were not removed and the energy from this source ranged from 2000 cm^{-1} to about 3000 cm^{-1}. The alignment lamps were the primary IR source used to verify interferometer alignment. The blackbody lamps served as a back-up IR source in the event the alignment lamps could not be used.

The two wideband sources were mounted near the front cover of the telescope and used to track the response of the interferometer to all optical elements in the telescope and interferometer. Energy from these two sources reflected from the front cover allowing it to enter the telescope and reach the interferometer.

The off-axis source was a small incandescent lamp installed in the baffles of the telescope. It was used to get some measure of the off-axis performance of the telescope if the cold surfaces of the telescope became contaminated and scattered energy into the interferometer. Unfortunately, the source was not bright enough and no changes in detector response were seen during flight.

2.8 Interferometer Signal Conditioning Electronics (ISCE)

The ISCE consisted of two functionally separated subsystems, which converted energy incident on the five interferometer detectors into electrical signals. Channels 1, 3, and 5 were processed by one ISCE. The second ISCE processed channels 2 and 4. This partitioning allowed part of the channels to continue processing data even if the sister ISCE experienced an anomaly that blocked the flow of IR data. Each channel employed separate electrical filtering and a 16-bit analog-to-digital converter to process the five interferogram signals. Each of the five channels had three selectable gain levels (X1, X10, and X100), a fixed gain of 1.75, and two bias level selections (medium and low).

The gain and bias of the five channels in the ISCE could be changed using three techniques. An automatic, microprocessor-based scheme was the primary method used to control the value of the gain and bias for each channel. The controlling microprocessor sampled the DC voltage of each detector and made changes to the detector's gain or bias, as required, to put in place that combination that would optimize the dynamic range of each channel. New gains or biases were put into place during the retrace period of the moving mirror.

In the second method of gain and bias control, the CIRRIS experiment sequencer controlled bias as part of a prescribed mission mode. The command sequencer sent commands to the gain ranging microprocessor to set the bias at low or medium, or leave it in its present state. The algorithm in the microprocessor retained control of electronic gain and could select any one of the three gains. This method was used primarily in backup modes stored in the Control and Monitor Panel (CMP) located on the AFD. These modes were available if the CIRRIS command sequencer developed a problem and was not able to produce the commands needed to configure for each measurement block.

The final gain ranging control mode was a manual mode in which the crew members could set any one of the three electronic gains or two bias levels in place on any channel. Manual operation was a contingency mode and was not used during the flight.

2.9 Carriage Lock

Electromagnetic locking was required to secure the MMC during launch and de-orbit to prevent any excessive stresses to the carriage. The locking force selected was about ten times the restoring force of the flex pivots. The electromagnet would attract a catch plate mounted on the carriage and hold it firmly against the interferometer's cube when the carriage was

brought back to the locking position. This secured the carriage and did not allow it respond to angular mechanical inputs. 2A flight-qualified lithium battery powered the lock.

Restraining the interferometer's moving mirror carriage (MMC) during the launch and descent phases of the flight was necessary to prevent any mechanical vibrations from interacting with the natural mechanical resonance of the carriage. Any rotational input frequency near 3 Hz could excite this resonance and cause the carriage to hit hard stops and perhaps suffer optical misalignment or damage to a flex pivot or other carriage component. Retaining alignment and mechanical integrity was crucial throughout launch, descent, and post-flight processing to accommodate the calibration effort that was scheduled post-flight.

The carriage was released when the interferometer was powered on. A relay removed power and the electromagnet was degaussed with a "ringing" circuit. A capacitor and resistor were placed in parallel with the coil of the electromagnet to cause a damped ringing waveform and remove any residual magnetism in the magnet or keeper.

3. MISSION INTERFEROMETER OPERATIONS

3.1 Interferometer Health Check

The first on-orbit task was to conduct a health check of the sensors to see how they had tolerated the launch. This activity was scheduled as measurement block PC32 at MET 0/09:03:00. In this block, the alignment of the interferometer, the integrity of the optical filters, and the NESRs for the five detectors were checked. The alignment was checked with the filter wheel in position 4, the alignment source on, and the short scan selected. Table 3 shows the in-flight NESR for each detector.

TABLE 3. FLIGHT NESR AND GOAL NESR

NESR on Orbit ($Wcm^{-2}sr^{-1}cm^{1}$ @ $10\mu m$)	Detector No.	
	1	3.3×10^{-14} ($8\ cm^{-1}$ scan in 1.53 sec)
	2	2.6×10^{-14} ($8\ cm^{-1}$ scan in 1.53 sec)
	3	6.7×10^{-14} ($8\ cm^{-1}$ scan in 1.53 sec)
	4	1.3×10^{-13} ($8\ cm^{-1}$ scan in 1.53 sec)
	5	Data not available

3.1 Sensor Contamination Control

Great care was taken to prevent any contamination of the CIRRIS telescope and the two IR sensors. The first scheduled measurement block (PC10) was delayed, by design, for nearly 23 hours to MET 0/22:45:00 to give the orbiter time to outgas any water or other contaminants prior to opening the telescope cover for the first time. The outgassing delay was later waived by three hours to start the first measurement block at MET 0/19:45 and take advantage of the extraordinary auroral activity observed by the crew.

Constraints on each measurement block set a waiting period between any release of propellent, water, or other substance and the start of CIRRIS measurements. This time was 90 minutes during the early mission and then reduced to 60 minutes during late mission as confidence grew. The constraints required that CIRRIS ops be scheduled after the dispersal period if a water dump, a fuel cell purge, flash evaporator operations, or PRCS firing had occurred. VRCS operations had to finish 10 minutes before the telescope cover opened and no RCS activity was allowed unless the telescope cover was closed. These constraints were effective and allowed the telescope and IR sensors to avoid the effects of contamination on the very cold surfaces inside the telescope.

3.2 Focal Plane Performance

The five detectors of the focal plane performed as expected throughout all phases of the flight. Very few spiking incidents have been seen in the interferometer's data base during post-flight data analysis. The spiking that has been observed falls into two categories. The first and most abundant type appear to be one-sample data dropouts with the point significantly different compared to the data points just before or after the event. The second type has two to six points in the spike. These spikes are closer to the average value of the data points nearby. The frequency of occurrence of the two types does not seem to be correlated with any particular geographic area. Data collected while the orbiter was in the South Atlantic Anomaly (SAA) has about the same number of spiking events compared to data collected away from that area. Interferograms collected in the SAA have the same exceptional quality found in data sets obtained in other areas.

Although the interferometer's focal plane was expected to operate at the 10° Kelvin temperature through all measurement blocks, early depletion of the cryogen supply[5] mandated some operations at an elevated focal plane temperature to continue taking interferometric data during the last measurement block. The temperature of the focal plane rose to about 13° with other optical components in the interferometer and telescope also at elevated temperatures. The interferometer still recorded good data during this block at the elevated temperatures.

3.3 Interferometer Alignment

In addition to unforseen causes of misalignment, early concerns focused on the possibility that the alignment system could, itself, produce a misalignment if the fixed mirror mechanical system responded to some unforseen vibration and moved away from the alignment point.

Through experience gained in the transportation of the CIRRIS experiment on the ground and in airplanes, it became evident that the optical components of the interferometer and the alignment system supporting the fixed mirror stayed in place during shipment, and the crew was advised there would probably be no loss of alignment during the launch. With the interferometer remaining in alignment during the launch, it was possible for the flight ops team to cancel that operational block set aside as a realignment contingency and to use the time to do measurement block (PC10A), thus taking advantage of the very active aurora occurring during this period of the timeline.

3.4 Vibration Constraints

The interferometer was very sensitive to vibration inputs during the integration period before flight. These inputs caused second-order distortion in the transformed interferograms.

Even though the interferometer's carriage was balanced as carefully as possible to make it unresponsive to linear inputs, the interferometer still reacted to angular inputs. Primarily, these inputs came from the movement of the interferometer's optical filter wheel and from the operation of the gimbal's pitch brake as it released and set. It was also expected that treadmill activity by the crew would create unwanted inputs.

The first two inputs were managed on-orbit by scheduling the movements of the filter wheel and the gimbal during the interferometer's retrace period. When the retrace period was not long enough to complete the operation, short scans were scheduled with the understanding that the data from these scans might be corrupted by the vibrational inputs.

Every attempt was made to schedule CIRRIS experimental operations at those times when treadmill exercise was not scheduled. A constraint was included in the flight plan to avoid scheduling treadmill and CIRRIS experiments at the same time. Except for one ten-minute period that occurred because of unavoidable concurrent scheduling, the interferometer's data escaped contamination by treadmill operations. During the ten-minute period, the data from the interferometer was markedly affected, thus illustrating the necessity of avoiding treadmill activities when interferometer measurements are in progress.

3.5 Electronic Upset

The CIRRIS interferometer suffered one electronics upset during the flight. The upset occurred at MET 0/23:59:00 during the second air glow block PC10B. Although the interferometer continued to take data in its default mode, tangent height and optical filter coordination was lost. The crew had been advised that electronic upset was likely to happen and they were extensively trained to handle this contingency. The episode lasted about 10 minutes until Lacy Veach was able to reset the interferometer's electronics and resume the measurement block.

No direct cause for the electronics upset has been determined. The orbiter was over Northern Florida when the episode started and well away from the South Atlantic Anomaly. Other electronics elements of the payload had experienced anomalies just before the interferometer electronics upset. After this upset, there were no other upsets of any of the electronic systems on the payload.

3.6 Laser Reference System

The two laser reference systems for the interferometer arrived on-orbit aligned and producing the same electrical signals measured during the closeout health check before launch. The reference system continued to work well throughout the flight, except for some self-heating that brought the temperature of the two boxes out-of-limits high. Responding to this anomaly, the two systems were alternately scheduled to allow the non-working laser to cool while the second laser supplied reference interferograms.

4. CONCLUSIONS

Discovery proved to be a good platform for collecting interferometric IR data on a global basis over an extended period of time. The sensors on board the shuttle were able to meet or exceed all expectations and conditions imposed by mission requirements. The shuttle environment did not markedly affect the performance of the sensor. Those items on the shuttle that produced contamination did not significantly impact any measurements. Scheduling, based on sensor constraints, was very successful in avoiding those operations of the shuttle that could have seriously degraded the performance of the interferometer.

Except for the one electronic upset, the interferometer successfully collected high-quality, high-resolution data for the 19 hours that the CIRRIS-1A experiment operated on-orbit. The CIRRIS interferometer successfully tolerated the launch and de-orbit environments with no loss of function or optical alignment. The sensor was found to be in alignment after the landing, and was successfully calibrated when it arrived back in Utah.

Acknowledgments

The work described in this paper was the result of the many contributions and individual efforts by members of SDL/USU staff and members of the staff of the Air Force Phillips Laboratory in Boston, Ma. Members of the Aerospace Corporation and Lockheed Missiles and Space Company also made many important suggestions that lead to the successful operation of the interferometer on-orbit. Notably, the work of John Kemp and Kent Johnson at SDL/USU in crafting the mechanical/optical components of the interferometer was most important to the success of the CIRRIS-1A experiment.

References

[1]Kemp, J.C. and Huppi R.J., "Rocket-borne Cryogenic Michelson Interferometer," Multiplex and/or High Throughput Spectroscopy, SPIE, Vol. 191, pp. 135-142, 1979.

[2]Kemp, J.C., Wellard, S.J., Goode, D.C., and Huppi, E.R., "Cryogenic Michelson Interferometer Spectrometer for Space Shuttle Application," SPIE, Vol. 686, pp. 151-159, 1986.

[3]Nadile, R.M., Et Al, "Observations of Infrared Atmospheric Emissions with the Cryogenic Infrared Radiance Instrumentation for Shuttle (CIRRIS 1A) from STS 39," American Geophysical Union, Dec 1991.

[4]Nadile, R.M., Et Al, "STS 39 Measurement of 4.3 μm Earth Limb Emissions from CO_2 and NO^+," American Geophysical Union, May, 1992.

[5]Bartschi, B., Steed, A., Blakeley, J., and Griffin, J., Cryogenic Infrared Radiance Instrumentation for Shuttle (CIRRIS 1A) Instrumentation and Flight Performance, submitted to SPIE, June, 1992.